Pathogens and Disease, 74, 2016, ftw033

doi: 10.1093/femspd/ftw033
Advance Access Publication Date: 17 April 2016
Research Article

RESEARCH ARTICLE

Fimbriae have distinguishable roles in *Proteus mirabilis* biofilm formation

Paola Scavone[1], Victoria Iribarnegaray[1], Ana Laura Caetano[1], Geraldine Schlapp[1], Steffen Härtel[2] and Pablo Zunino[1,*]

[1]Department of Microbiology, Instituto de Investigaciones Biológicas Clemente Estable, Montevideo 11600, Uruguay and [2]Laboratory for Scientific Image Processing (SCIAN-Lab), Biomedical Neuroscience Institute, Institute of Biomedical Sciences, Faculty of Medicine, University of Chile, Santiago 8380453, Chile

*Corresponding author: Department of Microbiology, Instituto de Investigaciones Biológicas Clemente Estable, Av. Italia 3318, Montevideo 11600, Uruguay. Tel: (+598) 24871616; Fax: (+598) 24875461; E-mail: pzunino@iibce.edu.uy

One sentence summary: *Proteus mirabilis* causes complicated urinary tract infections, especially those associated with catheterization; biofilm formation and different types of fimbriae are critical in this process, exerting particular effects.

Editor: Filip Ruzicka

ABSTRACT

Proteus mirabilis is one of the most common etiological agents of complicated urinary tract infections, especially those associated with catheterization. This is related to the ability of *P. mirabilis* to form biofilms on different surfaces. This pathogen encodes 17 putative fimbrial operons, the highest number found in any sequenced bacterial species so far. The present study analyzed the role of four *P. mirabilis* fimbriae (MR/P, UCA, ATF and PMF) in biofilm formation using isogenic mutants. Experimental approaches included migration over catheter, swimming and swarming motility, the semiquantitative assay based on adhesion and crystal violet staining, and biofilm development by immunofluorescence and confocal microscopy. Different assays were performed using LB or artificial urine. Results indicated that the different fimbriae contribute to the formation of a stable and functional biofilm. Fimbriae revealed particular associated roles. First, all the mutants showed a significantly reduced ability to migrate across urinary catheter sections but neither swimming nor swarming motility were affected. However, some mutants formed smaller biofilms compared with the wild type (MRP and ATF) while others formed significantly larger biofilms (UCA and PMF) showing different bioarchitecture features. It can be concluded that *P. mirabilis* fimbriae have distinguishable roles in the generation of biofilms, particularly in association with catheters.

Keywords: urinary tract infection; *Proteus mirabilis*; fimbriae; biofilm

INTRODUCTION

Proteus mirabilis is one of the most common etiological agents associated with catheter-associated urinary tract infections (CAUTIs) (Warren *et al.* 1982). The risk of having a urinary tract infection (UTI) increases up to 50% with short-term catheterization (up to 7 days) whereas all patients undergoing long-term catheterization (longer than 28 days) will develop bacteriuria (Morris and Stickler 1998).

Proteus mirabilis can form biofilms on catheter surfaces which lead to complications such as alteration in local pH through the production of urease, which hydrolyzes the urine urea. Ammonia production then raises the local pH allowing

Received: 30 September 2015; **Accepted:** 7 April 2016

Table 1. Bacterial strains used in this study.

Strain	Description	Relevant features	Reference
Pr2921	Clinical isolation from patient with UTI (parental strain)	Amp^S, Tet^R, Eri^R, Pol^R, swarming$^+$, hemolysin$^+$, urease$^+$	Zunino *et al.* 2000
MSD2	Isogenic *mrpA* mutant obtained by allelic replacement with *mrpA*:Km cassette	Amp^S, Tet^R, Eri^R, Pol^R, Km^R, swarming$^+$, hemolysin$^+$, urease$^+$	Zunino *et al.* 2001
P2	Isogenic *pmfA* mutant obtained by allelic replacement with a *pmfA*:Km cassette	Amp^S, Tet^R, Eri^R, Pol^R, Km^R, swarming$^+$, hemolysin$^+$, urease$^+$	Zunino *et al.* 2003
UM1	Isogenic *ucA* mutant obtained by allelic replacement with a *ucaA*:Km cassette	Amp^S, Tet^R, Eri^R, Pol^R, Km^R, swarming$^+$, hemolysin$^+$, urease$^+$	Pellegrino *et al.* 2013
A4	Isogenic *atfA-C* mutant obtained by allelic replacement with a *atfA-C*:Km cassette	Amp^S, Tet^R, Eri^R, Pol^R, Km^R, swarming$^+$, hemolysin$^+$, urease$^+$	Zunino *et al.* 2000

precipitation of minerals which deposit on the catheter biofilm forming what is known as a mineral encrustation (Jacobsen and Shirtliff 2011). Due to the deposition of crystals within these biofilms, blockage of the urinary catheter can occur causing retention of urine in the bladder and episodes of ascending UTI (Jones *et al.* 2007). Encrustration can cause trauma to the bladder mucosa and urethra upon removal of the catheter (Stickler and Zimakoff 1994).

Microbial biofilms have been defined as sessile communities characterized by cells that are irreversibly attached to a substratum or interface or to each other, embedded in a matrix of extracellular polymeric substances that they produce, which exhibit an altered phenotype compared to their planktonic counterparts (Donlan and Costerton 2002).

Bacterial biofilm formation is a complex process that depends on a wide range of genes (O'Toole, Kaplan and Kolter 2000). However, it is known that different surface proteins of bacterial cells may exert a key role in biofilm development. Particularly, *P. mirabilis* encodes 17 putative fimbrial operons, the highest number found in any sequenced bacterial species so far (Pearson *et al.* 2008). Contribution to infection of some of these structures has been assessed, but little is known about their contribution to catheter adherence and biofilm formation. The *P. mirabilis* fimbriae that have been most extensively studied are MR/P (mannose-resistant *Proteus*-like), PMF (*P. mirabilis* fimbriae), ATF (ambient temperature fimbriae) and UCA (uroepithelial cell adhesin) (Nielubowicz and Mobley 2010). MR/P, PMF and UCA fimbriae have been related to infection of the urinary tract by *P. mirabilis* and to adhesion to uroepithelial cells using different models while ATF mutagenesis did not affect infection ability when the ascending UTI model in the mouse was used (Zunino *et al.* 2000). Swarming motility is another distinctive characteristic of *P. mirabilis*, produced when short vegetative swimmer cells differentiate into elongated and highly flagellated swarmer cells (Rozalski, Sidorcyk and Kotelko 1996).

The aim of the present work was to analyze the contribution of *P. mirabilis* fimbriae in biofilm formation using different isogenic mutants unable to express MR/P, UCA, ATF and PMF fimbriae, generated in our laboratory. Biofilm production was evaluated using the semiquantitative adhesion assay to polystyrene plates and crystal violet staining while biofilm development in Luria Bertani (LB) broth or artificial urine over time was analyzed by immunofluorescence and confocal microscopy. Descriptors used for analysis of biofilms formed by the wild type and the mutants were biofilm biovolume and extracellular matrix volume. Also, migration of the different strains over catheter sections of different materials and swimming and swarming motility were assessed.

It has been shown in previous studies that *P. mirabilis* produced different biofilms depending on the growth media (Jones *et al.* 2007). Therefore, different assays were performed using LB broth or artificial urine, since this last medium has been proved to be useful in mimicking natural infection by *P. mirabilis* (McLean *et al.* 1985).

METHODS

Bacterial strains

Bacterial strains used in this study are listed in Table 1. All mutant strains derived from the clinical wild type *P. mirabilis* Pr2921 (Zunino *et al.* 2000). Bacteria were cultured in LB broth and when solid media were required 1.5% agar was added. Artificial urine (AU) was prepared according to Soriano *et al.* (2009) and contained the following compounds (in g L^{-1}): $CaCl_2$, 0.49; $MgCl_2$, 0.65; NaCl, 4.6; Na_2SO_4, 2.3; sodium citrate, 0.65; sodium oxalate, 0.02; KH_2PO_4, 2.8; KCl, 1.6; NH_4Cl, 1.0; urea, 25; and trypticase soy broth, 1.0. pH was adjusted to 6.2, and the AU was sterilized using a Millipore membrane of 0.45 μm pore size.

Growth curves

Bacterial suspensions were prepared in phosphate-buffered saline (PBS) from fresh LB agar plates at optical density (OD) at 540 nm = 0.1. Ten microliters of the bacterial suspension was transferred to microtitration 96-well plates containing 200 μl of LB or AU. Plates were incubated at 37°C with shaking and OD 540 nm was measured at different time points.

Swimming and swarming motility

To assess swimming motility, the different strains were inoculated by puncture into LB supplemented with 0.3% agar, as described by Hola, Peroutkova and Ruzicka (2012). Assays were performed six times and motility areas were measured and compared using the Student's t-test.

Swarming motility of the different strains was evaluated as described by Jones *et al.* (2004). Bacterial suspensions were prepared from fresh LB agar plates at a similar OD in PBS. After 18 h incubation in LB broth, 10 μl were placed on the center of LB agar plates. Inocula were dried at ambient temperature and then plates were incubated for 12 h at 37°C. The distance from

the center to the edge of migration was measured and the area of the ellipse calculated. This assay was performed three times and values were compared using the Student's t-test.

Bacterial migration over urethral catheters

Plates containing 12 ml of LB agar were dried at ambient temperature for 3 h and 1 cm channels were cut as described by Stickler and Hughes (1999). After drying, two aliquots of 10 μl of a 4 h culture were inoculated at the edge of the central channel of each plate. After the inocula dried on the agar, 1 cm silicone and latex catheter sections (Silkomed® and Silkolatex Rusch Gold, Teleflex Medical, Kernen, Germany) were placed as bridges. The plates were incubated at 37°C overnight and examined for swarming across the catheter bridge. Inocula were placed onto a separated section without a bridge as control. Each strain was assayed 15 times and the results were expressed as the number of times the strain crossed the catheter. Results were compared using the Chi-squared test.

Quantification of biofilm formation on polystyrene multiwell plates

Overnight LB cultures of the six strains were diluted (1/10) in fresh broth and dispensed in triplicate in sterile flat-bottomed polystyrene 96-well plates. After 48 h of incubation at 37°C, medium containing the planktonic cells was removed and three washes with PBS were performed. Quantification was assessed by adding 200 μl of 0.1% crystal violet (CV) for 15 min. Then the plates were washed with PBS in order to remove the dye excess. CV was solubilized with 95% ethanol and absorbance was measured at 590 nm (de los Santos *et al.* 2014). The absorbance values were considered as a measure of biofilm formation (Villegas *et al.* 2013). Results were compared using the Student's t-test.

Assessment of biofilm evolution over time by immunofluorescence

Biofilm formation was evaluated in LB and AU under static conditions at 37°C for 2, 5 and 7 days after inoculation as described previously (Schlapp *et al.* 2011). Briefly, 0.3 ml of overnight cultures in LB were used to inoculate tubes with 30 ml of LB or AU containing a sterile glass coverslip (Corning, NY 14831, USA). Biofilms were formed over the coverslip at the appropriate time point. Coverslips were first washed in PBS in order to remove planktonic cells and then fixed with 4% paraformaldehyde in PBS for 20 min. This step was done in order to kill bacteria and prevent biofilm growing over time. After that, coverslips were subjected to *in situ* immunofluorescence as described in Schlapp *et al.* (2011) with some modifications. A 15 min permeabilization step was performed after incubation with non-permeabilization buffer (NP; 2% bovine serum albumin in PBS, 0.05 M NH_4Cl, pH 7.2). Bacteria were stained with SYTO 9 (Molecular Probes®, Thermofisher, Waltham, MA, USA) and extracellular matrix with FilmTracer SYPRO® Ruby (Thermofisher, Waltham, MA, USA) biofilm matrix stain.

Image acquisition by confocal laser scanning microscopy

Acquisition of 3D image stacks was performed using a Leica TCS LSI super-zoom confocal fluorescence microscope with an iXon Ultra 897 back-illuminated imaging EMCCD camera, LAS Software, a ×100 oil immersion objective (NA = 1.35) and 488/520, 450/610 nm excitation/emission wavelength using software LASAF (Leica, Wetzlar, Germany). Three z-stacks were randomly chosen in each sample, using an acquisition step of 0.3 μm in the z-axis and 1024 × 1024 pixels in the *xy*-plane with a pixel size of 170 nm.

Image restoration and quantification of biofilm descriptors

3D image stacks were deconvolved with Huygens Software as described previously (Schlapp *et al.* 2011). Briefly, signal to noise ratio was adjusted until the deconvolved images were free of pixel noise. Image processing routines were applied on the basis of IDL 7.1 (Interactive Data Language, ITT, Boulder, Colorado, USA) using ScianSoft for segmentation, visualization, 3D reconstruction and determination of biofilm descriptors. Segmentation of individual bacteria was performed as described previously (Schlapp *et al.* 2011). For matrix segmentation we applied the scaling index method (Räth and Morfill 1997), a pixel-wise non-linear transformation in combination with a threshold value that we modified previously with a weighting vector (Härtel *et al.* 2005). Bacterial volume and extracellular matrix volume of biofilms were calculated from the region of interest (ROI) data after segmentation. Bacterial volume was calculated considering the voxels (μm^3) for each bacteria (Schlapp *et al.* 2011) and the sum of all bacterial volumes were calculated for each strain and condition. Results were analysed using the Duncan's new multiple range test.

RESULTS

Bacterial growth in different media

Growth curves of bacteria cultured in LB and AU showed a similar behavior among the different strains ($P > 0.05$ in every case, Fig. 1). However, we observed that higher values of absorbance were reached in LB broth (Fig. 1a) compared to AU (Fig. 1b).

Swimming and swarming motility

Swimming motility of the mutants did not show any significant difference compared with the wild type when growth surfaces were measured (Table 2). The wild type strain generated a swimming motility area of 49.23 ± 7.79 cm^2 and the mutant values ranged from 30.27 ± 16.09 cm^2 (MR/P mutant MSD2) to 42.73 ± 12.83 cm^2 (PMF mutant P2).

The results of swarming motility are shown in Table 2. The swarming motility area generated by the wild type strain Pr2921 was 50.27 ± 0.10 cm^2 while the mutant swarming surfaces ranged from 28.27 ± 0.10 (UCA mutant UM1) to 43.01 ± 12.70 cm^2 (PMF mutant P2). Differences between the wild type and mutant swarming areas were not significant in any case.

Migration across catheter bridges

The influence of different fimbriae on bacterial migration across catheter sections (latex and silicone) was evaluated (Table 2). The wild type (Pr2921) strain was able to cross both types of catheter in every case (15 bridges). Fimbrial mutants showed different abilities to cross the bridges, depending on the catheter materials. However, all the fimbrial mutants showed a significant impairment in their catheter bridge migration capacity when either latex or silicone sections were used (Table 2).

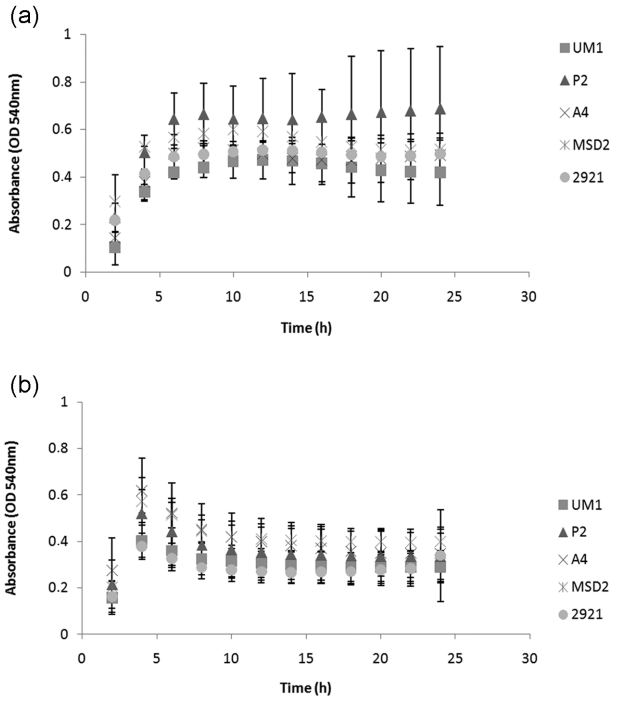

Figure 1. Growth curves of Pr2921 *P. mirabilis* wild type strain and UCA, PMF, ATF and MR/P fimbrial mutants (UM1, P2, A4 and MSD2, respectively). Symbols and bars represent mean values and standard deviation (SD), respectively. **(a)** Growth curves generated by serial OD measurements of bacteria grown in LB broth. **(b)** Growth curves generated by serial OD measurements of bacteria grown in artificial urine.

Biofilm formation on polystyrene and CV staining

The effect of the different mutations in biofilm formation was evaluated using the semiquantification technique based on absorption of associated CV. The mutant strains showed different abilities to form biofilms in LB (Fig. 2a). MR/P mutant (MSD2) showed the lowest biofilm formation value (Fig. 2) and was significantly reduced compared to the rest of the strains. The ATF mutant (A4) exhibited a moderate biofilm formation ability, also significantly smaller than the wild type strain (Pr2921) (Fig. 2a). On the other hand, UCA and PMF mutants (UM1 and P2, respectively) formed significantly larger biofilms than the MR/P mutant although differences were not significant compared with the wild type (Fig. 2a).

Biofilms formed in AU were in general smaller compared to biofilms produced in LB (Fig. 2b). All the mutants exhibited a significantly impaired capacity to form biofilms compared with the wild type except the PMF mutant (P2) (Fig. 2b).

Biofilm development over time

Biofilm formation and bioarchitecture over time was evaluated in static cultures in LB broth and AU at 37°C at 2, 5 and 7 days after inoculation, using confocal laser scanning microscopy (CLSM) and image analysis.

When biofilm formation in LB broth was assessed after 2 days, the wild type strain showed a significantly higher bacterial volume compared with the rest of the strains (Figs 3a, and 4a and b). At this time point, the UCA (UM1) mutant strain showed a significant increase of biofilm extracellular matrix volume compared with the other mutants strains (Fig. 3b). In AU at day 2, the ATF mutant (A4) was the only strain able to adhere to the coverslip (Fig. 3c). This mutant strain was the only one that also produced extracellular matrix in this medium at this time point (Fig. 3d).

At day 5, UCA (UM1) and PMF (P2) mutant strains showed a significant increase in their bacterial volume in LB, and these values were significantly higher compared with the wild type, ATF (A4) and MRP (MSD2) mutant strains (Fig. 3a).

At this time point, the wild type Pr2921 and PMF (P2) mutant exhibited a strong production of biofilm extracellular matrix, while a significant decrease was detected in the rest of the mutants compared to the wild type (Fig. 3b). In AU, after 5 days, all the strains were attached to the surface and no significant bacterial volume differences were detected between them or when compared to the wild type (Fig. 3c). Also, no significant differences in extracellular matrix production were detected between the wild type and the mutant strains (Fig. 3d).

At day 7, the strains that showed the highest values of total bacterial volume in LB were the wild type Pr2921 and UCA (UM1) mutant strain (Fig. 4c and d, respectively). However, differences were not significant when compared with the other strains (Fig. 3a). Regarding matrix volume, wild type Pr2921, UCA (UM1) and PMF (P2) mutant strains were the highest producers but again these differences were not significant compared with the rest of the mutants (Fig. 3b). After 7 days in AU, all the mutants except PMF (P2) showed a significant decrease in biofilm total bacterial volume compared to wild type Pr2921 (Figs 3c, and 4e and f). The PMF (P2) mutant was also the highest extracellular matrix producer under these conditions and this value was significant compared with all the strains, including wild type (Pr2921). The other mutants did not exhibit significant differences compared with the wild type (Fig. 3d).

DISCUSSION

Proteus mirabilis is a well known cause of complicated UTI, with a special incidence in catheterized patients. This pathogen can

Table 2. Bacterial ability to migrate across urinary catheter sections, and swimming and swarming motility.

Strain	Latex (%, P)	Silicone (%, P)	Swimming (cm^2) (P)[a]	Swarming (cm^2) (P)[a]
Pr2921	15/15 (100%)	15/15 (100%)	49.23 ± 7.79	50.27 ± 0.10
MSD2	11/15 (73%, 0.03)	8/15 (53%, 0.0025)	30.27 ± 16.09 (0.28)	31.37 ± 19.29 (0.14)
P2	5/15 (33%, 0.0001)	9/15 (60%, 0.0062)	42.73 ± 12.83 (0.34)	43.01 ± 12.70 (0.46)
UM1	11/15 (73%, 0.03)	9/15 (60%, 0.0062)	37.99 ± 18.42 (0.18)	28.27 ± 0.10 (0.06)
A4	2/15 (13%, <0.0001)	10/15 (66%, 0.014)	39.81 ± 14.55 (0.31)	34.21 ± 12.70 (0.17)

Strains used in this assay were Pr2921 wild type strain and UCA, PMF, ATF and MR/P fimbrial mutants (UM1, P2, A4 and MSD2, respectively).
[a]P values were calculated comparing motility areas of the wild type and each mutant.

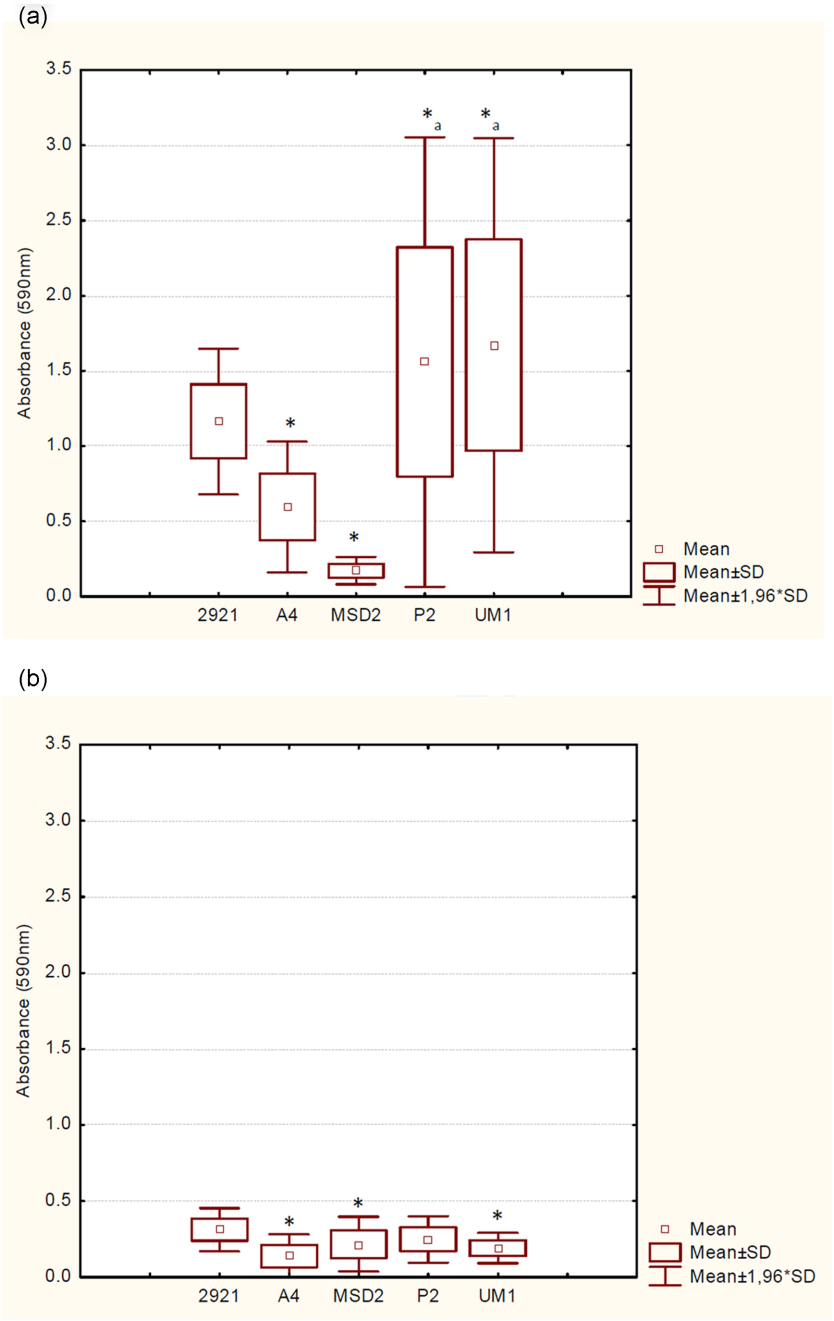

Figure 2. Biofilm formation on polystyrene surfaces assessed by the semiquantitative method based on crystal violet staining. Pr2921 *P. mirabilis* wild type strain and UCA, PMF, ATF and MR/P fimbrial mutants (UM1, P2, A4 and MSD2, respectively) were grown in LB broth (**a**) and in artificial urine (**b**). * indicates significant differences compared to all the other strains. *a indicates significant differences compared to the other strains but not between each other.

form dense crystalline biofilms that block catheters, causing severe complications in affected patients (Stickler 2014).

In a previous study we reported that uropathogenic *P. mirabilis* biofilm is generated through a coordinated and well-defined morpho-topological process (Schlapp *et al.* 2011). In that study we measured different parameters obtained from CLSM images, revealing that features such as number of bacteria, bacterial volume and volume of extracellular matrix or bacterial compaction varied over time following a characterizable pattern. In this work we used a set of fimbrial mutants to assess the role of these surface structures in *P. mirabilis* in migration over urinary catheters and biofilm formation.

In the present study it could be observed that the four different fimbriae assessed were relevant for bacterial migration on catheter sections. It is important to note that all the single fimbrial mutations showed an impaired ability to migrate, confirming the important roles of these structures in biofilm associated with catheter colonization. However, the swimming and swarming motility of any of the mutants was not significantly affected compared to the wild type. This suggests that the impairment of migration on catheters of the different fimbrial mutants is based on the lack adhesion but not on alteration of bacterial motility. In previous assays, we could observe that an isogenic flagellar mutant (Scavone *et al.* 2015) could not migrate through catheter

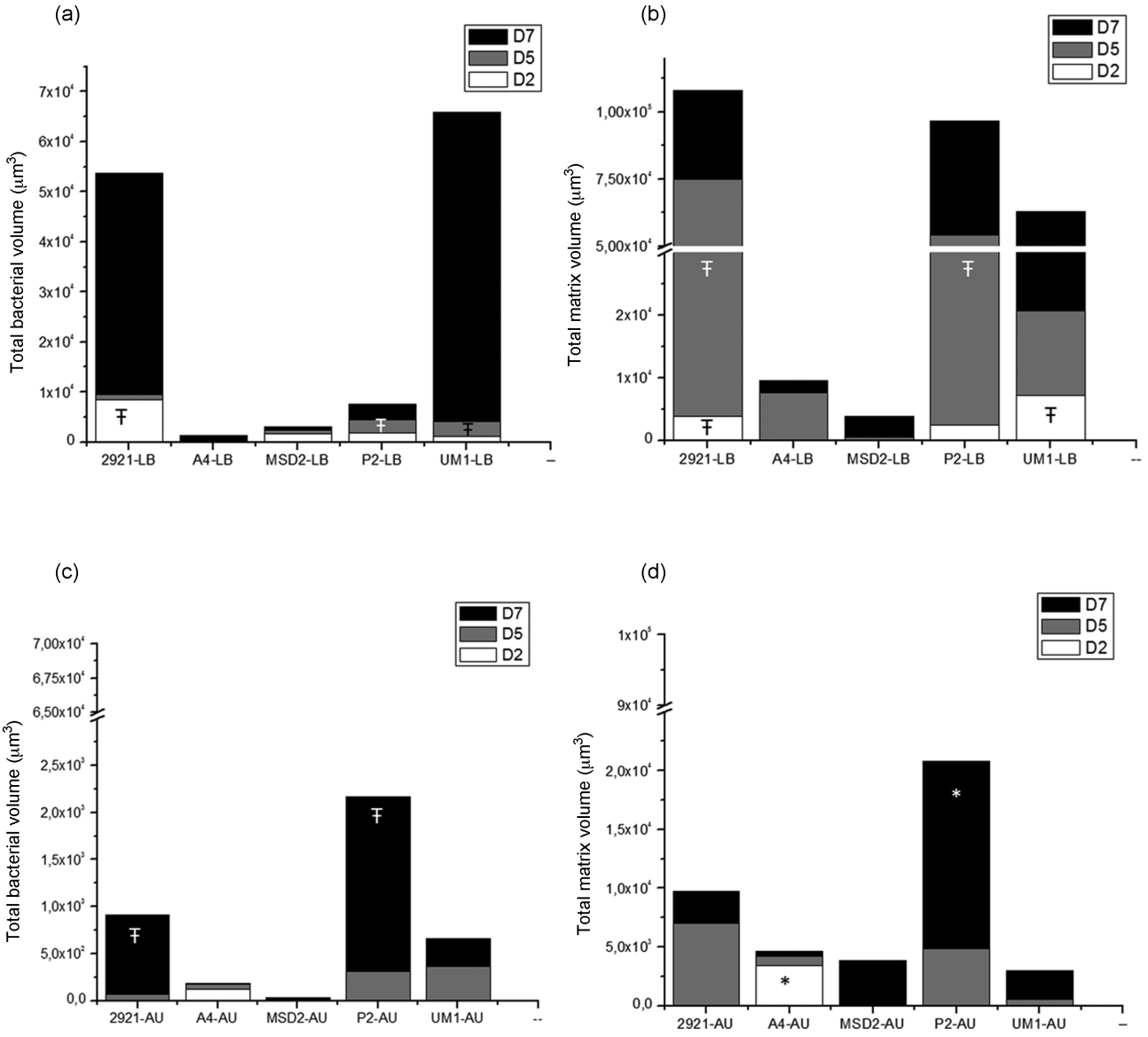

Figure 3. Total bacteria and matrix volumes in biofilms formed by *P. mirabilis* in LB broth and in artificial urine (AU). Pr2921 *P. mirabilis* wild type strain and UCA, PMF, ATF and MR/P fimbrial mutants (UM1, P2, A4 and MSD2, respectively) grown in LB broth (**a** and **b**) and in AU (**c** and **d**). * indicates significant differences compared with all the other strains. Ŧ indicates significant differences compared with the other strains but not between each other.

sections of different materials and was non-motile as expected (data not shown). These results confirm that the impairment of fimbrial mutants to migrate over the catheter sections is related to adhesion but not to motility. This finding would seem to be relevant since fimbriae could be considered as potential targets to control UTI associated with catheterization (Guiton *et al.* 2012).

Motility results also suggest that polar effects due to the mutated genes were not seen. In *P. mirabilis* motility and adhesion through flagella and fimbriae are coregulated events. For example, the *mrpJ* gene in the MR/P fimbriae operon encodes a transcriptional regulator that represses swimming and swarming and is also involved in several other cellular process, becoming a global regulator (Bode *et al.* 2015). Moreover, in *P. mirabilis* there are several *mrpJ* paralogues, most of them associated with fimbrial operons (Pearson and Mobley 2008).

To corroborate the absence of polar effects associated with the mutations, we analysed the expression of fimbrial downstream genes by real-time RT-PCR. Fimbrial gene expression was observed in all the mutants (data not shown) confirming the absence of a polar effect associated with the mutations.

To assess the influence of environmental factors on biofilm formation, particularly medium composition, bacterial development in LB broth and artificial urine (AU) was evaluated. In general, bacterial growth was similar between the wild type and the mutants but growth in AU was reduced since values were about one-half compared to LB broth, confirming that the environment has a strong influence on *P. mirabilis* biofilms (Jones *et al.* 2007). Although the formation of micro-crystals in this medium due to *P. mirabilis* urease activity (approximately after 10–12 h) may interfere with readings, growth curves of the wild type strain and the mutants were similar,

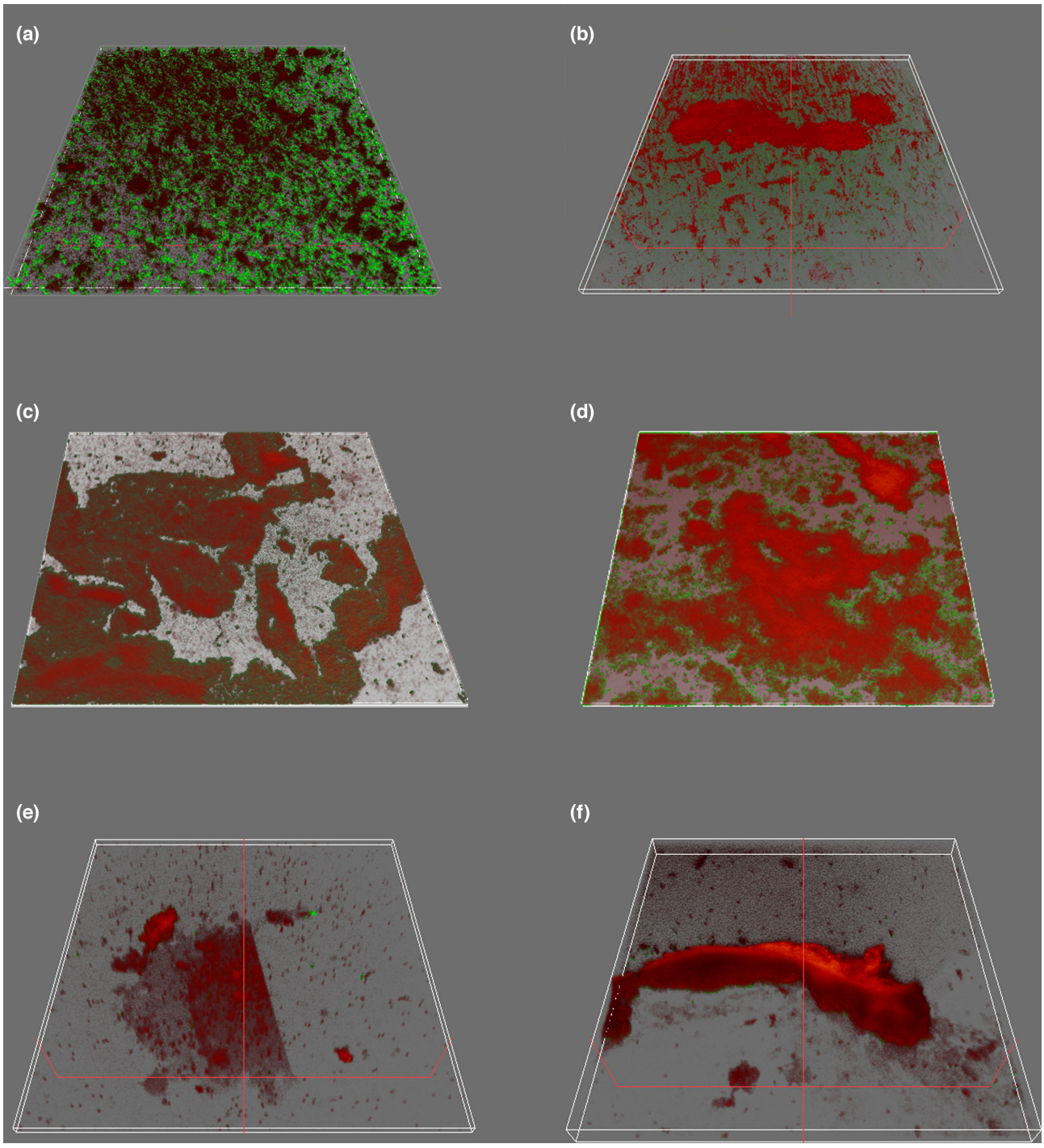

Figure 4. 3D reconstruction of biofilms. Bacteria are represented in green and matrix in red. (**a**) Pr2921 *P. mirabilis* wild type strain and (**b**) UCA mutant strain (UM1) biofilm after 2 days of culture in LB. (**c**) Pr2921 *P. mirabilis* wild type strain and (**d**) UCA mutant strain (UM1) biofilm after 7 days of culture in LB. (**e**) Pr2921 *P. mirabilis* wild type strain and (**f**) PMF mutant strain (P2) biofilm after 7 days of culture in AU.

When biofilm formation was assessed using the semiquantitative method based on CV staining, MR/P and ATF mutants showed a significant smaller biofilm compared with the wild type when grown in LB broth. However, the UCA and PMF mutants formed larger biofilms than the wild type. When bacteria were grown in AU for this assay, all the mutants formed smaller biofilms, except P2 (PMF mutant). Interestingly, the ATF mutant was the most affected strain, grown either in LB broth or in AU. In a previous study we had reported that ATF did not have a role in experimental *P. mirabilis* UTI (Zunino *et al.* 2000). These results were associated with optimal expression of this fimbria at ambient temperature (Massad, Bahrani and Mobley 1994). Results obtained here suggest that ATF fimbriae, among others, could have a role in adhesion and biofilm formation on abiotic surfaces; in addition they do not have an apparent role in urovirulence.

CLSM revealed that when bacteria were grown in LB broth, the effects of the different mutations in biofilm formation varied over time. Regarding bacterial volume, a significant decrease was observed only at early stages (2 days) in the case of all the fimbrial mutants. However, after 5 days, bacterial volumes of UCA and PMF mutants significantly increased compared to the wild type. After 7 days, the UCA mutant still exhibited the highest bacterial volume biofilms although differences were not significant compared to the wild type. MR/P and ATF mutants (MSD2 and A4, respectively) exhibited a significant decrease of extracellular matrix at different time points. These results confirm that fimbriae are important factors that contribute to biofilm ultrastructure and stability, as reported for other organisms (Hung *et al.* 2013).

When CLSM was used to assess biofilm formation in AU, the main result was that bacterial biovolume of the fimbrial mutants, except PMF, showed a significant decrease compared to the wild type at day 7. Also, at that time point, PMF mutant extracellular matrix significantly increased while the rest of the mutants did not show significant changes compared to the wild type. Also, this mutant exhibited the highest biofilm bacterial volume. Results showed that the different fimbrial mutants have a role in reaching normal biofilm parameters, except the PMF mutant, which formed significantly enhanced biofilm biomass.

Our results confirm that the UCA and, in particular, the PMF mutant, form enhanced biofilms compared to the wild type. Probably, these fimbriae contribute to the control of the formation of stable and functional biofilms. Similar situations have been reported by Holling *et al.* (2014) in the case of several transposon *P. mirabilis* mutants that exhibited the formation of enhanced biofilm biomass. On the other hand, MR/P and ATF mutants formed significantly smaller biofilms than the wild type strain. Interestingly, a fimbria such as ATF that does not have an apparent role in UTI may be important in biofilm formation on abiotic surfaces.

Overall, although certain redundant effects between different fimbriae cannot be ruled out, the present study strongly suggests that *P. mirabilis* fimbriae have distinguishable roles in the generation of functional biofilms, particularly associated with catheters.

FUNDING

This work was supported by grant FCE 104760 awarded by ANII-Uruguay and PEDECIBA-Uruguay. SH is supported by FONDECYT 1151029, FONDEF D11I1096 ANILLO ACT 10712 and ICM P09-015-F.

Conflict of interest. None declared.

REFERENCES

Bode NJ, Debnath I, Kuan L *et al.* Transcriptional analysis of the MrpJ network: modulation of diverse virulence-associated genes and direct regulation of *mrp* fimbrial and *flhDC* flagellar operons in *Proteus mirabilis*. *Infect Immun* 2015;**83**: 2542–56.

de los Santos R, Fernández M, Carro S *et al.* Characterisation of *Staphylococcus aureus* isolated from cases of bovine subclinical mastitis in two Uruguayan dairy farms. *Arch Med Vet* 2014;**46**:315–20.

Donlan R, Costerton J. Biofilms: survival mechanisms of clinically relevant microorganisms. *Clin Microbiol Rev* 2002;**15**: 167–93.

Guiton P, Cusumano C, Kline K *et al.* Combinatorial small-molecule therapy prevents uropathogenic *Escherichia coli* catheter-associated urinary tract infections in mice. *Antimicrob Agents Chemother* 2012;**56**:4738–45.

Härtel S, Rojas R, Räth C *et al.* Identification and classification of di- and triploid erythrocytes by multi-parameter image analysis: a new method for the quantification of triploidization rates in rainbow trout (*Oncorhynchus mykiss*). *Arch Med Vet* 2005;**37**:147–54.

Hola V, Peroutkova T, Ruzicka F. Virulence factors in *Proteus bacteria* from biofilm communities of catheter-associated urinary tract infections 2012. *FEMS Immunol Med Microbiol* 2012;**65**:343–9.

Holling N, Lednor D, Tsang S *et al.* Elucidating the genetic basis of crystalline biofilm formation in *Proteus mirabilis*. *Infect Immun* 2014;**82**:1616–26.

Hung C, Zhou Y, Pinkner J *et al.* *Escherichia coli* biofilms have an organized and complex extracellular matrix structure. *MBio* 2013;**4**:e00645–13.

Jacobsen S, Shirtliff M. *Proteus mirabilis* biofilms and catheter-associated urinary tract infections. *Virulence* 2011;**2**: 460–5.

Jones B, Young R, Mahenthiralingam E *et al.* Ultrastructure of *Proteus mirabilis* swarmer cell rafts and role of swarming in catheter-associated urinary tract infection. *Infect Immun* 2004;**72**:3941–50.

Jones S, Yerly J, Hu Y *et al.* Structure of *Proteus mirabilis* biofilms grown in artificial urine and standard laboratory media. *FEMS Microbiol Lett* 2007;**268**:16–21.

McLean R, Nickel J, Noakes V *et al.* An *in vitro* ultrastructural study of infectious kidney stone genesis. *Infect Immun* 1985; **49**:805–11.

Massad G, Bahrani FK, Mobley HL. *Proteus mirabilis* fimbriae: identification,isolation, and characterization of a new ambient-temperature fimbria. *Infect Immun* 1994;**62**:1989–94.

Morris N, Stickler D. Encrustation of indwelling urethral catheters by *Proteus mirabilis* biofilms growing in human urine. *J Hosp Infect* 1998;**39**:227–34.

Nielubowicz G, Mobley H. Host–pathogen interactions in urinary tract infection. *Nat Rev Urol* 2010;**7**:430–41.

O'Toole G, Kaplan H, Kolter R. Biofilm formation as microbial development. *Annu Rev Microbiol* 2000;**54**:49–79.

Pearson M, Sebaihia M, Churcher C *et al.* Complete genome sequence of uropathogenic *Proteus mirabilis*, a master of both adherence and motility. *J Bacteriol* 2008;**190**: 4027–37.

Pearson MM, Mobley HL. Repression of motility during fimbrial expression: identification of 14 *mrpJ* gene paralogues in *Proteus mirabilis*. *Mol Microbiol* 2008;**69**:548–58.

Pellegrino R, Scavone P, Umpiérrez A *et al.* *Proteus mirabilis* uroepithelial cell adhesin (UCA) fimbria plays a role in the colonization of the urinary tract. *Pathog Dis* 2013;**67**:104–7.

Räth C, Morfill G. Texture detection and texture discrimination with anisotropic scaling indices. *J Opt Soc Am A* 1997;**14**: 3208–15.

Rozalski A, Sidorcyk Z, Kotelko K. Potential virulence factors of *Proteus* bacilli. *Microbiol Mol Biol Rev* 1996;**61**:65–89.

Scavone P, Villar S, Umpiérrez A *et al.* Role of *Proteus mirabilis* MR/P fimbriae and flagella in adhesion, cytotoxicity and genotoxicity induction in T24 and Vero cells. *Pathog Dis* 2015;**73**, DOI: 10.1093/femspd/ftv017.

Schlapp G, Scavone P, Zunino P *et al*. Development of 3D architecture of uropathogenic *Proteus mirabilis* batch culture biofilms—A quantitative confocal microscopy approach. *J Microbiol Methods* 2011;**87**:234–40.

Soriano F, Huelves L, Naves P *et al*. *In vitro* activity of ciprofloxacin, moxifloxacin, vancomycin and erythromycin against planktonic and biofilm forms of *Corynebacterium urealyticum*. *J Antimicrob Chemother* 2009;**63**:353–6.

Stickler D. Clinical complications of urinary catheters caused by crystalline biofilms: something needs to be done. *J Intern Med* 2014;**276**:120–9.

Stickler D, Hughes G. Ability of *Proteus mirabilis* to swarm over urethral catheters. *Eur J Clin Microbiol Infect Dis* 1999;**18**:206–8.

Stickler D, Zimakoff J. Complications of urinary tract infections associated with devices used for long-term bladder management. *J Hosp Infect* 1994;**28**:177–94.

Villegas N, Baronetti J, Albesa I *et al*. Relevance of biofilms in the pathogenesis of Shiga-toxin-producing *Escherichia coli* infection. *ScientificWorldJournal* 2013;**2013**:607258.

Warren J, Tenney J, Hoopes J *et al*. A prospective microbiologic study of bacteriuria in patients with chronic indwelling urethral catheters. *J Inf Dis* 1982;**146**:719–23.

Zunino P, Geymonat L, Allen A *et al*. Virulence of a *Proteus mirabilis* ATF isogenic mutant is not impaired in a mouse model of ascending urinary tract infection. *FEMS Immunol Med Microbiol* 2000;**29**:137–44.

Zunino P, Geymonat L, Allen A *et al*. New aspects of the role of MR/P fimbriae in *Proteus mirabilis* urinary tract infection. *FEMS Immunol Med Microbiol* 2001;**31**:113–20.

Zunino P, Sosa V, Allen A *et al*. *Proteus mirabilis* fimbriae (PMF) are important for both bladder and kidney colonization in mice. *Microbiology* 2003;**149**:3231–7.